

Collisional radiative modeling on optical emission spectroscopy for Ar plasma

Duck-Hee Kwon*, Kil-Byoung Chai

Nuclear Data Center, Korea Atomic Energy Research Institute, Daejeon 34057, Republic of Korea

*Corresponding author: hkwon@kaeri.re.kr

1. Introduction

Optical plasma diagnostic methods such as optical absorption and emission, laser-induced fluorescence, Raman and Thomson scattering have been extensively used to measure electron/ion temperature and density, species concentrations in plasmas [1]. Optical emission spectroscopy (OES) is comparatively simple, versatile, non-intrusive, and has been widely used. The OES has been utilized to gas discharge low-temperature plasmas such as capacitively coupled plasma (CCP) and inductively coupled plasma (ICP) for their numerous applications in analytical chemistry and microelectronic processing [2-4].

OES determines plasma parameters by line ratio method combined with population kinetics modeling. General model for the population kinetics taking into account all possible collisional and radiative processes of atoms and ions in plasma are called collisional-radiative model (CRM). We have carried out an OES and CRM for a CCP system and the spectroscopic results for Ar plasma depending on gas pressure, applied rf power and electron temperature/density are presented and analyzed.

2. Methods and Results

2.1 CRM

Populations (n_i) of the i levels are obtained by solving the stationary rate balance equations:

$$\sum_{j \neq i} n_e n_j \alpha_{ji}^{ex} + \sum_{j > i} \eta_{ji} A_{ji} = \sum_{j \neq i} n_e n_j \alpha_{ij}^{ex} + \sum_{j < i} \eta_{ij} A_{ij} + n_e n_i \alpha_i^{iz} + n_i \nu_i^d,$$

where n_e is the volume averaged electron density, α_{ij}^{ex} is the electron impact excitation/deexcitation rate coefficient from i th level to j th level, α_i^{iz} is the electron impact ionization rate coefficient for i th level, A_{ij} and η_{ij} are transition probabilities (Einstein's A coefficient) and escape factor for optical transition, from ν_i^d is the quenching probability per unit time by diffusion to chamber walls. Fig. 1 illustrates the energy levels and reaction processes included in the

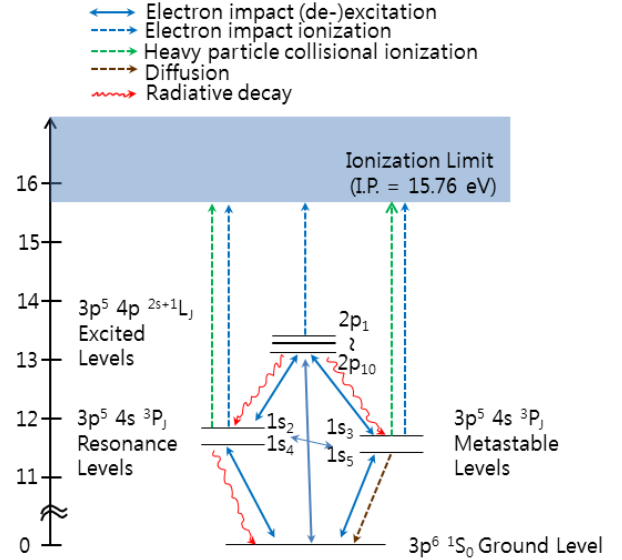


Fig. 1. Energy levels and reaction processes considered in present CR modeling for Ar. Pachen notations are also given for the levels.

Table I: Wavelengths (nm) and transition probabilities (A_{ij} , 10^8sec^{-1}) in parentheses for dipole allowed radiative decays of Ar I.

Excited Levels	Resonance Levels		Metastable Levels	
	1s ₂ (J=1)	1s ₄ (J=1)	1s ₃ (J=0)	1s ₅ (J=2)
2p ₁ (J=0)	750.39 (0.45)	667.73 (0.002)		
2p ₂ (J=1)	826.45 (0.15)	727.29 (0.02)	772.42 (0.12)	696.54 (0.06)
2p ₃ (J=2)	840.82 (0.22)	738.40 (0.08)		706.72 (0.04)
2p ₄ (J=1)	852.14 (0.14)	747.12 (0.0003)	794.82 (0.19)	714.70 (0.006)
2p ₅ (J=0)	858.01	751.47 (0.40)		
2p ₆ (J=2)	922.45 (0.05)	800.62 (0.05)		763.51 (0.25)
2p ₇ (J=1)	935.42 (0.01)	810.37 (0.25)	866.79 (0.02)	772.38 (0.05)
2p ₈ (J=2)	978.45 (0.01)	842.46 (0.22)		801.48 (0.009)
2p ₉ (J=3)				811.53 (0.33)
2p ₁₀ (J=1)	1148.8 (0.002)	965.78 (0.05)	1047.0 (0.01)	912.30 (0.19)

CRM. Table 1 lists the optical transition wavelengths and the transition probabilities.

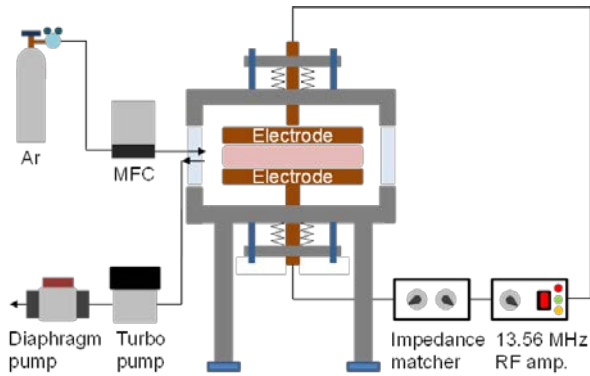


Fig. 2. Sketch of the experimental setup.

2.2 Experimental setup

A sketch of the experiment setup is shown in Fig. x; a conventional capacitively-coupled discharge source consisting of two parallel electrodes, a cylindrical vacuum chamber, a 13.56 MHz rf generator (YSR-06AF, Youngsin RF), and an automatic impedance matcher (AMN-100A, Youngsin RF). The copper electrodes are placed inside vacuum chamber with a gap distance of 0-4 cm (the gap distance was fixed at 3 cm in this work) and the radius of the electrodes is 3 cm. The radius of the vacuum chamber is 15 cm and the height is 15 cm. Plasmas are typically ignited by using the rf power of 1-20W. The typical operation pressure ranges from 20 mTorr to few hundreds of mTorr (measured by capacitance manometer).

In order to measure the plasma emission spectra, an Ocean Optics HR4000 spectrometer is used. The grating of the spectrometer has 300 grooves per mm and the width of the entrance slit is 5 microns. For collecting visible light photons, we use a specially designed collecting optics consisting of a cylindrical tube with baffle structures and a 2 inch bi-convex lens ($f=7.5$ cm). The collection optics is placed in front of the vacuum chamber window satisfying $2f-2f$ condition (15 cm away from both the plasma center and the fiber end). The spectroscopic system measured from 400 nm to 850 nm and the FWHM is about 0.3-0.4 nm. The OES setup was absolutely calibrated at the Korea Research Institute of Standards and Science (KRISS) using a quartz tungsten-halogen lamp and an integration sphere. To measure the electron temperature and density as well as electron energy probability function (EPPF), an RF compensated Langmuir probe (Impedans Ltd.) was used. The radius and length of the tungsten probe tip are 0.25 mm and 12 m, respectively. The measurement position is the radial and vertical center of the plasma.

2.3 Results

Fig. 3 shows the results of our CRM benchmarking previous OES and CRM for Ar plasma of pulsed DC magnetron [5] where the applied power is 1 kW, gas

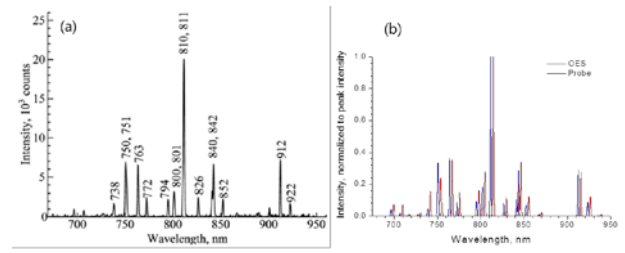


Fig. 3. Benchmark results in (b) of present CRM for a measured spectra [6] in (a). The blue line in (b) represents our CRM spectra for $T_e=7.37$ eV and $n_e = 3.15 \times 10^{10} \text{ cm}^{-3}$ determined from CRM by K. E. Evdokimov et al. [6]. The red line in (b) represents our CRM spectra for $T_e=7.86$ eV and $n_e=9.44 \times 10^{11} \text{ cm}^{-3}$ determined from probe measurement by K. E. Evdokimov et al. [6].

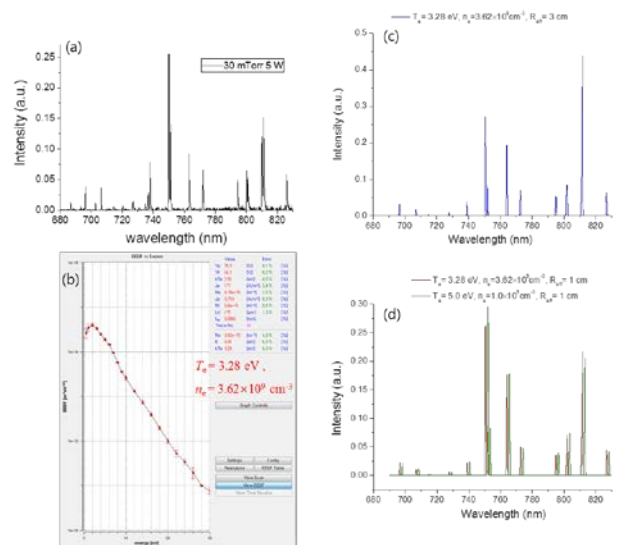


Fig. 4. (a) Measured spectra and (b) electron temperature and density from our CCP. (c) Our CRM spectra for $T_e=3.28$ eV and $n_e=3.62 \times 10^9 \text{ cm}^{-3}$ determined from probe measurement for effective plasma length R_{eff} assumed as chamber radius $R=3.0$ cm. (d) Our CRM spectra for $T_e=3.28$ eV, $n_e=3.62 \times 10^9 \text{ cm}^{-3}$ (red line) and $T_e=5.0$ eV, $n_e=1.0 \times 10^9 \text{ cm}^{-3}$ (green line) with $R_{\text{eff}}=1.0$ cm .

pressure 0.45 mtorr (0.06 Pa), gas temperature $T_g = 493$ K, and effective plasma characteristic length $R_{\text{eff}} = 13.5$ cm . Our CRM spectra agree with their measured spectra [5] but shows a bit discrepancy when the electron temperature and density from the probe measurement was used in the CRM as shown in Fig. 3 similar to their CRM result

Fig. 4 shows the CRM results for our ,measured spectra in the CCP. When T_e and n_e by the probe measurement is used in the CRM with the effective plasma length R_{eff} assumed as the chamber radius, the modeled spectra shows large discrepancy with the

measured spectra shown in Fig. 4 (a) and (c). The CRM line intensity of 750 nm wavelength is smaller than those of 811 nm wavelength unlike the measured spectra. When reduced R_{eff} is used in the CRM, the agreement between the measured and the modeled spectra is improved as shown in Fig. 4 (a) and (d). Such CRM behavior depending on R_{eff} is also reported in other publication for a CCP system [6].

3. Conclusions

CRM including atomic processes in low temperature Ar plasma generated in a CCP chamber has been constructed and used to analyze spectra measured. Some discrepancies for specific transition lines between modeling and measurement may come from the detailed atomic data [7,8] underlying in the CRM and the sensitivity of line intensity to the atomic data will be investigated. Effect of EEPF and radiation trapping on the CRM in CCP will be also discussed by considering relevant plasma dynamics more rigorously.

REFERENCES

- [1] V. M. Donnelly, Plasma Diagnostics vol 1 Discharge Parameters and Chemistry, Sandiego: Academic, pp.1-46, 1989.
- [2] J.A.C. Broekaert, Analytical Atomic Spectrometry with Flames and Plasmas, second ed. Wiley-VCH, Weinheim, 2005.
- [3] M. A. Liebermann, A. J. Lichtenberg, Principles of Plasma Discharges and Materials Processing, second ed. John Wiley & Sons, Inc., New York, 2005.
- [4] M. Krachler, R. Alvarez-Sarandes, G. Rasmussen, High-Resolution Inductively Coupled Plasma Optical Emission Spectrometry for $^{234}\text{U}/^{238}\text{Pu}$ Age Dating of Plutonium Materials and Comparison to Sector Field Inductively Coupled Plasma Mass Spectrometry, Anal. Chem., Vol. 88, p. 8862, 2016.
- [5] K. E. Evdokimov et al., Study of Argon Ions Density and Electron Temperature and Density in Magnetron Plasma by Optical Emission Spectroscopy and Collisional-Radiative Model, Resource-Efficient Technologies, Vol. 3, p. 187, 2017.
- [6] S. Siepa et al., On the OES Line-ratio Technique in Argon and Argon-containing Plasmas, J. Phys. D: Appl. Phys., Vol. 47, 445201, 2014.
- [7] S. Iordanova, I. Koleva, Optical Emission Spectroscopy Diagnostics of Inductively-driven Plasmas in Argon Gas at Low Presures, Spectrochimica Acta Part B, Vol. 62, p.344, 2007.
- [8] See <http://nl.lxcat.net>